ELSEVIER

Polymer 41 (2000) 6403–6413

polymer

Rheological and dielectric studies of aggregation of barium titanate particles suspended in polydimethylsiloxane

D. Khastgir[a], K. Adachi[b,*]

[a]*Rubber Technology Centre, Indian Institute of Technology, Kharagpur, 721 302, India*
[b]*Department of Macromolecular Science, Graduate School of Science, Osaka University, Toyonaka, Osaka, 560-0043, Japan*

Received 27 July 1999; received in revised form 21 October 1999; accepted 8 November 1999

Abstract

Viscoelastic and rheo–dielectric properties were investigated for suspensions composed of barium titanate ($BaTiO_3$) particles having an average size of 0.3 μm and polydimethylsiloxane (PDMS). Steady shear viscosity decreased with increasing shear rate. Stepwise increase of shear rate resulted in a thixotropic decrease of the viscosity due to reorganization of aggregates of the $BaTiO_3$ particles in the shear field. The transient change occurred through the fast and slow processes with the time constants of 5–30 and ca 100 s, respectively. Yield stress and plasticity were also observed for suspensions of high $BaTiO_3$ content. Since $BaTiO_3$ particles possess a strong dipole moment due to spontaneous polarization, the suspensions exhibited dielectric dispersion due to reorientation of the particles. The dielectric constant decreased with increasing viscosity of PDMS due to the increase of the dielectric relaxation time in the viscous medium. In order to investigate the aggregation of the particles in a shear field, we also carried out rheo–dielectric measurements in shear fields. The dielectric constant in a shear field decreased with increasing shear rate. After sudden stop of shear flow, a recovery of the dielectric constant was observed and was resolved into the fast and slow processes. The characteristic time for the fast process was close to the relaxation time for the thixotropy. Those results were explained by assuming chain-like aggregates of $BaTiO_3$ particles formed by the dipole–dipole interactions.

Keywords: Viscoelasticity; Barium titanate; Polydimethylsiloxane

1. Introduction

Polymers containing colloidal particles exhibit non-linear rheological behaviour and have been studied long from purely academic interests and also for the purpose of applications in industries of paints, foods, cosmetics, and processing of composite polymeric materials [1,2]. A variety of suspensions are known to exhibit non-linear viscoelastic behaviour such as shear thinning, thixotropy, rheopexy and dilatancy [3,4]. These behaviour are generally explained in terms of break-up of aggregates of colloidal particles under a shear field [5–9], i.e. the size and structure of the aggregates change depending on the shear rate. Frequently, aggregation and aggregates are called flocculation and flocs, respectively. In order to clarify the microscopic mechanism of the non-linear processes, we need to obtain information on the mobility and the structure of aggregated particles in a shear field. For this purpose, various techniques were employed such as computer simulation and rheo–optical methods [4,8]. In this study, we have applied the dielectric relaxation spectroscopy to a system composed of bariumtitanate ($BaTiO_3$) suspended in polydimethylsiloxane (PDMS) to clarify the relationship between the rheological properties and the structure of $BaTiO_3$ particles aggregated in the suspensions.

It is well known that $BaTiO_3$ is a ferroelectric crystal and exhibits spontaneous polarization [10]. Merz [11] reported the temperature dependence of the dielectric constant for a single crystal of $BaTiO_3$ which exhibits four crystalline modifications. The three low-temperature phases existing below 390 K possess a spontaneous polarization. Therefore, we expect that the particles of $BaTiO_3$ suspended in a medium exhibit dielectric relaxation as observed for polar molecules and that the dielectric behaviour reflects the size and structure of the aggregates. In the present study, we have attempted to investigate the structure and mobility of the $BaTiO_3$ particles by means of the dielectric method. Rheo–dielectric behaviour of the suspensions has been also investigated to observe the aggregate structure and dynamics of the $BaTiO_3$ particles in a shear field by using

* Corresponding author. Tel.: +81-66-850-5464; fax: +81-66-850-5464.
E-mail addresses: khasdi@rtc.iitkgp.ernet.in (D. Khastgir); adachi@chem.sci.osaka-u.ac.jp (K. Adachi).

0032-3861/00/$ - see front matter
PII: S0032-3861(99)00840-X

Table 1
Viscosity η of polydimethylsiloxane samples at 290 K

Code	η (poise)
t-PDMS-10	11[a]
PDMS-10	9.8
PDMS-100	96.2
PDMS-1000	950

[a] Reported by the manufacturer.

a rheo–dielectric apparatus reported previously [12]. From these viscoelastic and dielectric measurements, we investigated the effects of aggregation on the non-linear viscoelastic behaviour of the $BaTiO_3$/PDMS suspensions.

2. Experimental

2.1. Materials and sample preparation

Powder of $BaTiO_3$ was obtained from Wako Chemicals Co. Polydimethysiloxanes (PDMS) with different viscosities and a telechelic polydimethylsiloxane (t-PDMS) together with the crosslinking reagent were purchased from Shinetsu Chemicals Co. (Code; KE103). The sample code and viscosity of the PDMSs are given in Table 1. The scanning electron micrographs of the $BaTiO_3$ powder were taken with an electron microscope (JEOL JSM-5800) as shown in Fig. 1. It is seen that several $BaTiO_3$ particles form an aggregate. Although the resolution is poor, we see that the shape of each particle is close to cube or sphere and the size is 0.1–0.5 μm. Prescribed amount of the $BaTiO_3$ powder and PDMS were mixed and stirred vigorously for a few hours. Air bubbles were removed by evacuation. We used suspensions containing 50, 44, 37.5, 28.6 and 16.7 wt% of $BaTiO_3$, and the volume fractions ϕ of $BaTiO_3$ in these suspensions were 13.7, 11.7, 9.06, 6.23 and 3.12 vol%, respectively. Suspensions thus prepared are coded as BT(13.7)/t-PDMS-10 which indicates that the $BaTiO_3$ content ϕ is 13.7 vol% and the matrix is t-PDMS-10.

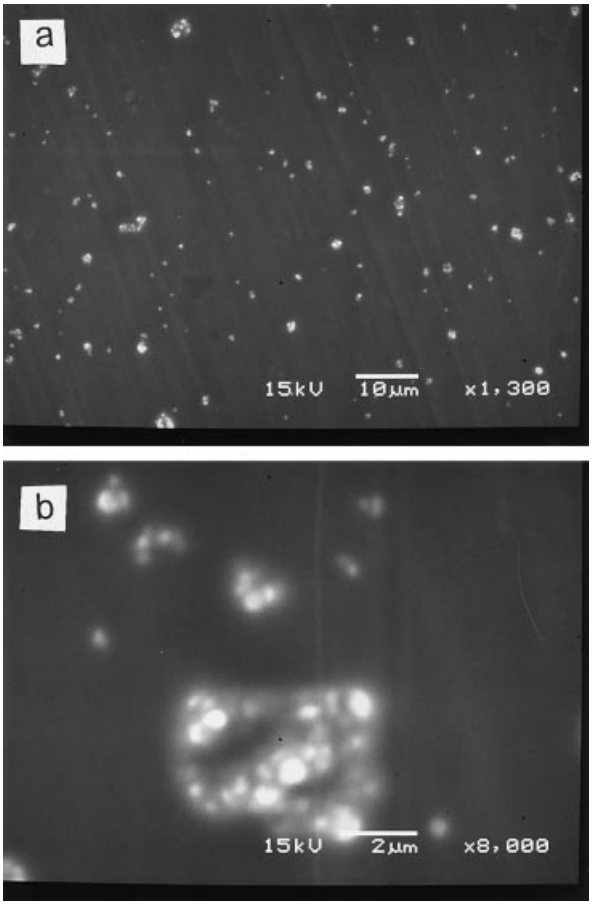

Fig. 1. Scanning electron micrograph of $BaTiO_3$ particles at: (a) low magnification; and (b) high magnification. A drop of a suspension of $BaTiO_3$ particles in dichloromethane containing 0.1 wt% of PDMS-1000 was put on a piece of aluminium film and the solvent was evaporated. PDMS-1000 was added to fix the particles on the film.

2.2. Method

Complex dielectric constant $\varepsilon' - i\varepsilon''$ in the audio-frequency range was measured with an RLC digibridge (QuadTech 1693). Dielectric measurements in low-frequency region were made by measurements of current with an amplifier (Keithley model 427). Steady-state viscosity η and complex shear modulus $G' + iG''$ were measured using a cone and plate type viscometer (Iwamoto IR200). In order to investigate the dielectric behaviour in a shear field, we also used a co-axial cylinder-type electrodes. The inner bob rotated at a regulated speed, and ε' and ε'' were measured with an LCR meter (Hewlett-Packard 4284A). Details are reported previously [12].

3. Results and discussion

3.1. Rheological behaviour

3.1.1. Steady viscosity

Fig. 2a shows the shear rate $\dot{\gamma}(= d\gamma/dt)$ dependence of steady-state viscosity η for the systems of t-PDMS-10 containing varying amount of $BaTiO_3$. In Fig. 2b, the η versus $\dot{\gamma}$ curves for the suspensions of PDMS-1000 and t-PDMS-10 containing 13.7 vol% of $BaTiO_3$ are shown. As is seen in these figures, η decreases with increasing $\dot{\gamma}$. Shear thinning behaviour has been reported by many authors for various suspensions and emulsions [2–5]. Such a thinning behaviour has been explained by considering change of the size of aggregates in a shear field.

First we compare the present result with the behaviour of suspensions of non-aggregating colloids. Zero shear viscosity η of a suspension of hard spheres is given by the Einstein–Batchelor equation [13]:

$$\eta = \eta_0(1 + 2.5\phi + 6.2\phi^2) \quad (1)$$

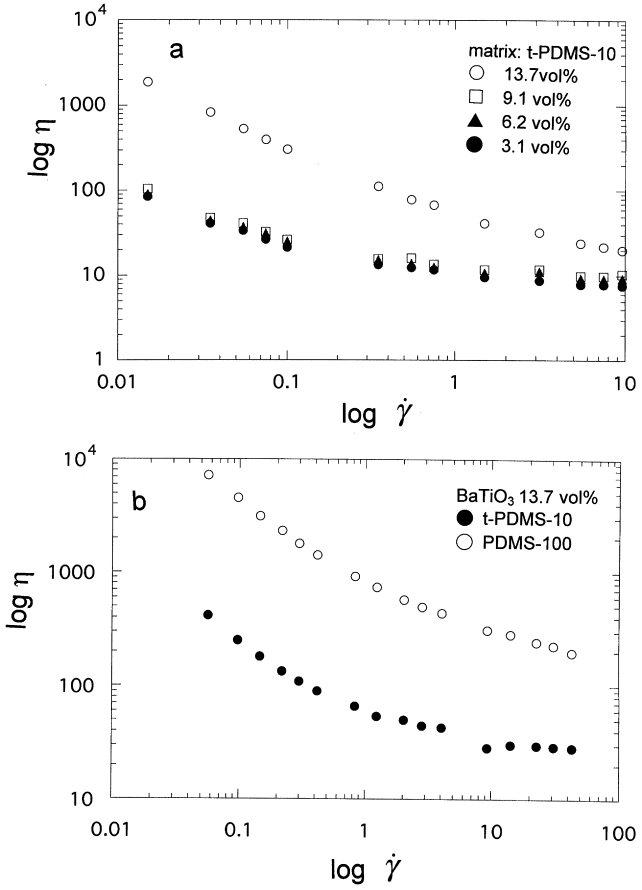

Fig. 2. Shear rate dependence of steady shear viscosity η for: (a) BT/t-PDMS-10 system with various $BaTiO_3$ contents indicated in the figure at 290 K; and (b) that for BT(13.7)/t-PDMS-10 and BT(13.7)/PDMS-1000.

where η_0 and ϕ are the viscosities of the medium and the volume fraction of the particles. It is known that for suspensions of hard spheres, Eq. (1) holds good in the range of $\phi < 0.1$ [6].

In Fig. 2a, we see that η of suspensions of $\phi < 0.1$ depends weakly on $BaTiO_3$ content. At the highest shear rate of $\dot{\gamma} = 10\ s^{-1}$, the viscosity value is close to that of the medium and agrees approximately with Eq. (1). This indicates that at $\dot{\gamma} = 10$ and $\phi < 0.1$, the particles form compact aggregates in which the effective volume fraction ϕ_{eff} of the aggregates is almost independent of the size of aggregates. In the range of low $\dot{\gamma}$, the size of aggregates becomes large and each aggregate contains non-free draining space in which the PDMS molecules cannot freely pass through. Thus ϕ_{eff} increases with decreasing $\dot{\gamma}$ below $10\ s^{-1}$. It is expected that aggregates have a self-similar structure as suggested by many authors [14,15].

In Fig. 2a, we also see that the viscosities of suspensions with $\phi < 0.1$ decrease slightly with ϕ. We cannot explain this weak ϕ dependence of η in the range of low $\dot{\gamma}$. Probably, interactions between the aggregates are weak and hence ϕ_{eff} does not change with the $BaTiO_3$ content. In suspension of 13.7 vol%, η is much higher than expected from Eq. (1). This suggests that a transition of the fractal structure of aggregates occurs around 10 vol% concentration.

In the above analyses, the shear thinning of the matrix PDMS has not been taken into account. Ito et al. reported that PDMS with the zero shear viscosity of 10 poise exhibits non-linear behaviour in the range of $\dot{\gamma} > 1000$ [16]. Therefore, the non-linear viscosity observed in Fig. 2a is mainly due to $BaTiO_3$ particles. However, in $BaTiO_3$/PDMS-1000, the non-linear behaviour seen in Fig. 2b is due to both effects of aggregation and medium viscosity. In Fig. 2b, it is seen that the $\dot{\gamma}$ dependence of η for suspensions in PDMS-10 is stronger than that in PDMS-1000.

Generally, it is well known that in colloidal suspensions, aggregates of particles are formed under a balance of electrical repulsion and van der Waals attractive force [5,6]. For the present system, we expect that additional dipole–dipole interactions play an important role for the formation of aggregates as in suspensions of ferromagnetic particles in which the magnetic dipole–dipole interaction among the particles is significant [17,18]. The interaction energy U between two point dipole vectors μ_1 and μ_2 is given by

$$U = -\frac{3(\mathbf{r}\mu_1)(\mathbf{r}\mu_2) - \mu_1\mu_2|\mathbf{r}|^2}{4\pi\varepsilon_0\varepsilon_m|\mathbf{r}|^5} \quad (2)$$

where $\mathbf{r}$ is the distance vector, ε_0 the dielectric constant of vacuum and ε_m, the relative dielectric constant of the medium. From the data of spontaneous polarization ($= 1.6 \times 10^{-1}\ C/m^2$) of $BaTiO_3$ [10,11], μ of a $BaTiO_3$ particle with the size of 0.3 μm is estimated to be 4.3×10^{-21} Cm, if the particle is composed of single polarization domain. Then, the interaction energy U for the case that two particles contact with head-to-tail configuration becomes -5.1×10^{-12} J. This value is ca 1.2×10^9 times larger than thermal energy k_BT at 300 K. We expect that the $BaTiO_3$ particles contain several polarization domains which are oriented so that the polarizations are cancelled. Thus, the dipole–dipole interaction is much smaller than the value calculated above. However, $BaTiO_3$ particles can be expected to form strong aggregates by the dipole–dipole interactions.

Linear aggregates due to the induced dipole moment is well known as the Winslow effect [19]. When a colloidal suspension is subjected to a strong electric field, the particles in the suspension are polarized and on account of the induced dipole moment, the particles tend to form a chain-like aggregates oriented in the direction of electric field [19–21]. Computer simulations have also indicated linear aggregates [22,23].

These facts suggest that $BaTiO_3$ particles in the present system form chain-like aggregates even in the absence of an electric field since the particles have a strong permanent dipole moment. In fact, we see in Fig. 1b that the aggregates have a coiled structure. Thus, the shear thinning behaviour observed in Fig. 2 can be explained by considering both extension and break-up of coiled aggregates in a shear

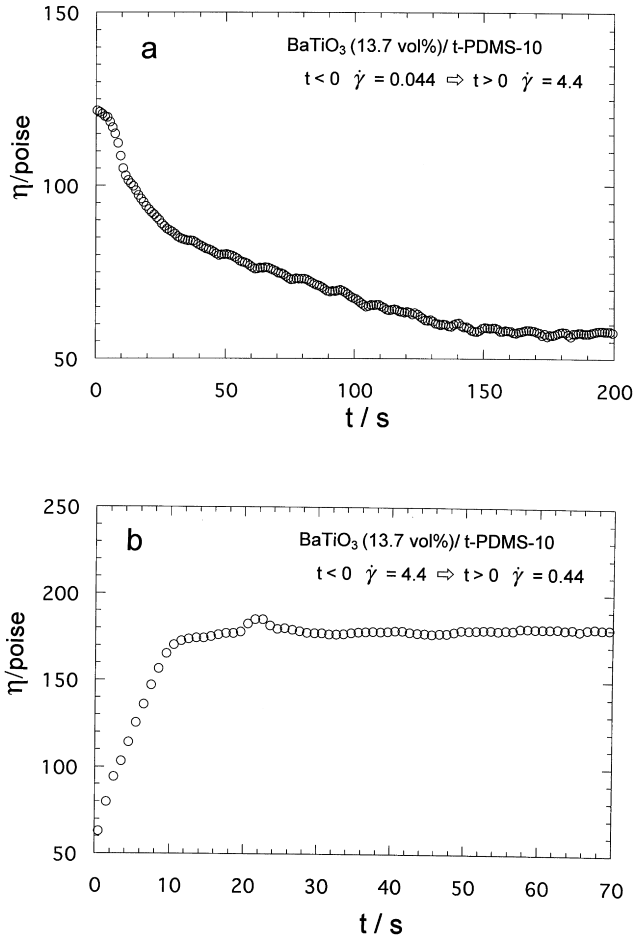

Fig. 3. Time dependence of shear viscosity after the stepwise change of shear rate at 290 K for BT(13.7)/t-PDMS-10 from: (a) 0.044–4.4 s^{-1}; and (b) 4.4–0.44 s^{-1}.

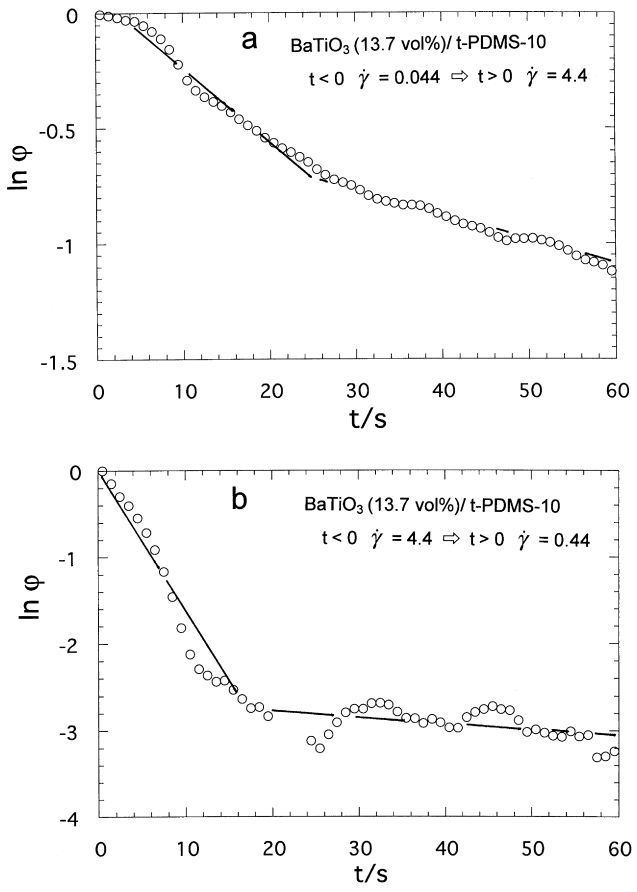

Fig. 4. Plot of the logarithm of φ(t) given by Eq. (3) for the data shown in Fig. 3.

field. We also expect that aggregates form a network structure when the concentration of particles is high as the viscosity of 13.7 vol% suspensions tends to diverge with decreasing shear rate as shown in Fig. 2.

3.1.2. Time dependence of viscosity

One of the characteristic features of colloidal suspensions is strong time dependence of η after a stepwise change of $\dot{\gamma}$, namely thixotropy and rheopexy [4]. In the present system, such behaviour was also observed. A representative example is shown in Fig. 3a for BT(13.7)/t-PDMS-10 which was subjected to a shear field of $\dot{\gamma} = 0.044\ s^{-1}$ and subsequently to a shear field of $\dot{\gamma} = 4.4$ at time $t = 0$. Fig. 3b shows the reverse case for observation of rheopexy: $\dot{\gamma}$ was decreased from 4.4 to 0.44. When $\dot{\gamma}$ is increased aggregates are broken into a smaller size and hence η decreases. Conversely, the decrease of $\dot{\gamma}$ results in the increase of η due to the recovery of the aggregate structure.

The transient variation of viscosity after the stepwise change of $\dot{\gamma}$ was fitted to a single retardation equation given by

$$\eta(t) - \eta(0) = \Delta\eta\varphi(t) \tag{3}$$

where $\eta(0)$ is the steady-state viscosity before the change of $\dot{\gamma}$; $\Delta\eta$ the total change of the viscosity, and $\varphi(t)$ the decay function. Examples of test of Eq. (3) are shown in Fig. 4a and b where the data of η shown in Fig. 3a and b are used, respectively. We see that $\varphi(t)$ is not single exponential. We resolved $\varphi(t)$ into two processes, namely the fast and slow. The time constants τ for the fast and slow processes of the thixotropic process (Fig. 4a) are 38 and 92 s, respectively, while those for the rheopexy (Fig. 4b) are 5.0 and 120 s, respectively. The time constants τ for the other suspensions were similar to those values but changed slightly from sample to sample. This scatter of time constant is probably due to experimental error especially for the slow process. On an average, τ for the fast and slow processes were of the order of 10 and 200 s, respectively.

For BT(13.7)/t-PDMS-10, measurements of η were performed in both directions of increasing and decreasing $\dot{\gamma}$. As is seen in Fig. 5, the system exhibited hysteresis. In contrast to the behaviour of most of suspensions, η increased after being subjected to a high shear. The hysteresis suggests that there exist the other slow relaxation

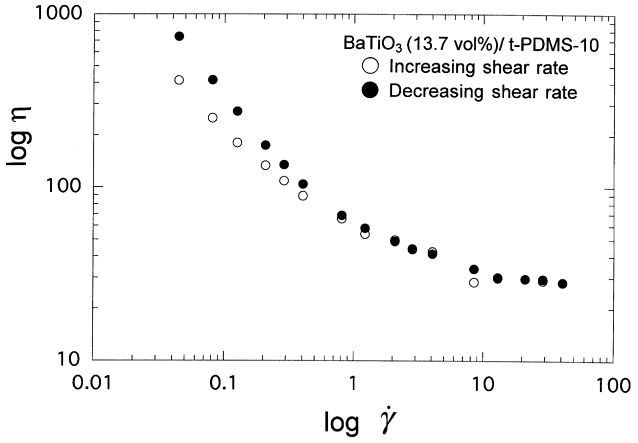

Fig. 5. An example of the hysteresis in viscosity measurement. Double logarithmic plot of viscosity versus shear rate at 290 K for BT(13.7)/t-PDMS-10.

processes through which the structural reorganization of aggregates is achieved very slowly in a shear field.

3.1.3. Plasticity

Fig. 6 shows the time dependence of the transient viscosity η (= stress S divided by $\dot{\gamma}$) after BT(13.7)/t-PDMS-10 is subjected to a shear field of 2.24 and 22.4 s^{-1}. As is seen in this figure, η exhibits an overshoot when $\dot{\gamma}$ is low. This indicates that BT(13.7)/t-PDMS-10 is a plastic body and has a network structure at a stationary state. For suspensions of lower concentration, such an overshoot was not observed. In order to examine the plasticity of suspensions, we used the Casson equation [24–26]:

$$\sqrt{S} = k_0 + k_1\sqrt{\dot{\gamma}} \quad (4)$$

where S is the shear stress, k_0 the square root of the yield stress and k_1 is the constant. Fig. 7 shows the plot of $S^{1/2}$ against $\dot{\gamma}^{1/2}$ for suspensions in t-PDMS-10 with varying $BaTiO_3$ content. It is seen that suspensions containing 13.7 vol% of $BaTiO_3$ exhibit clearly yield stress. On the other hand, the value of k_0 for suspensions with $BaTiO_3$ content less than 9 vol% is almost zero indicating that suspensions of $\phi < 0.1$ do not exhibit yield stress. The square of k_0 for BT(13.7)/PDMS-1000 was higher than BT(13.7)/t-PDMS-10 and was 225 dyn/cm^2.

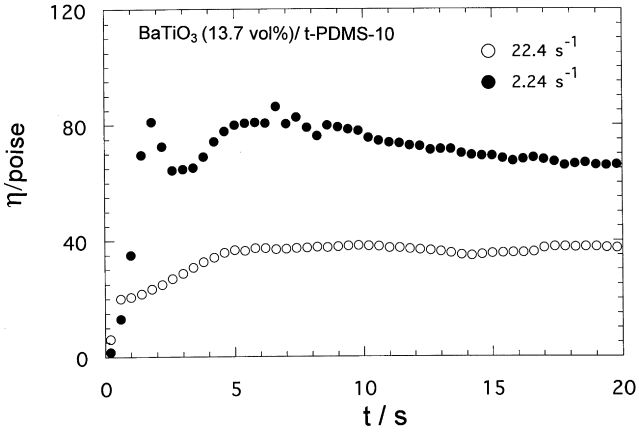

Fig. 6. Transient change of shear force S divided by the shear rate for BT(13.7)/t-PDMS-10 after the start of shearing at $t = 0$. The shear rate were 2.24 and 22.4 s^{-1}.

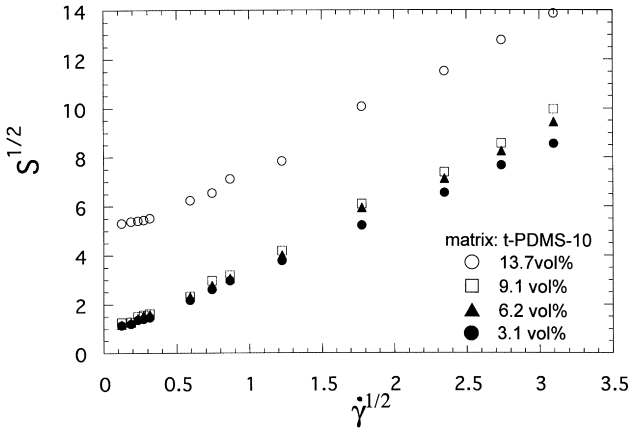

Fig. 7. Casson plot (Eq. (4)) for the system of BT/t-PDMS with varying content of $BaTiO_3$. (Replot of the data shown in Fig. 2a)

3.1.4. Dynamic shear moduli

The dynamic measurements were also carried out. An example of the Lisergue diagram of the shear stress versus shear strain at an amplitude of strain of 1.0 is shown in Fig. 8 for BT(13.7)/t-PDMS-10. The shape is not ellipsoidal indicating non-linear behaviour. Unfortunately, in our apparatus the amplitude of strain could not be reduced and therefore linear behaviour was not observed. In order to assess the dynamic shear modulus G, we defined G by $(a^2 - b^2)^{1/2}$ where a is the maximum value of S and b is the value of S at $\gamma = 0$. Fig. 9 shows the frequency dependence of G thus calculated. We see behaviour of so called second plateau over a wide frequency region [3]. These data indicate that aggregation of $BaTiO_3$ particles extends over a macroscopic size and forms a network-like structure. We speculate that some particles form islands or branches (see Fig. 17). Reorientation of these can be reflected to the dielectric relaxation as mentioned in the next section. Under a shear field, the network structure is broken into aggregates and the average size of these, decreases with increasing shear rate.

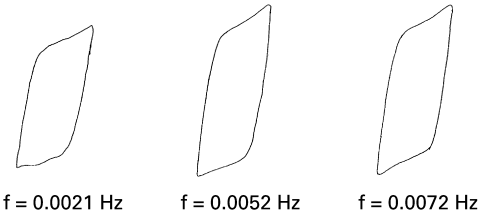

Fig. 8. Lissajous's diagrams of stress versus strain in measurements of dynamic shear modulus for BT(13.7)/t-PDMS-10.

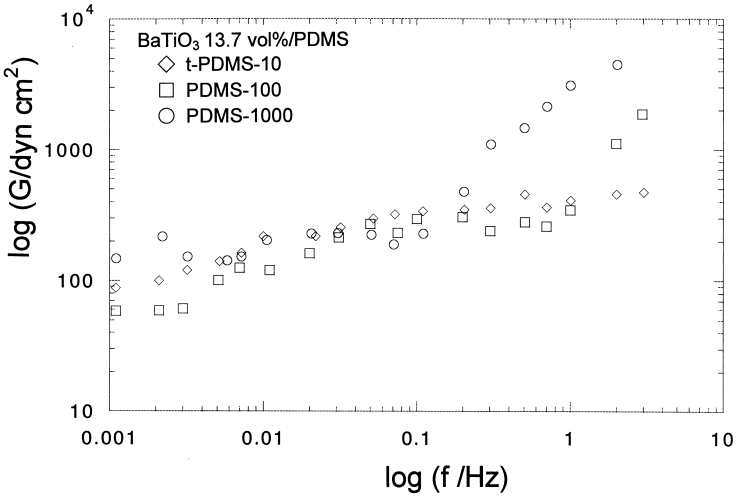

Fig. 9. Frequency f dependence of dynamic shear moduli G for the BT(13.7)/PDMS systems.

3.2. Dielectric behaviour

3.2.1. Temperature dependence of ε' and ε''

Temperature dependence of the dielectric constants ε' and loss factors ε'' for BT(9.1)/t-PDMS-10 are shown in Fig. 10a and b, respectively. In this figure, various dielectric anomalies can be seen. Among them the dielectric dispersion around 160 K is due to the primary dispersion of PDMS and the changes of ε' and ε'' at 240 K are due to melting of PDMS crystal [27]. On the other hand, the broad and strong dispersion around 300 K is due to $BaTiO_3$.

3.2.2. Dependence of ε' and ε'' on viscosity of PDMS

Here, we focus our attention to the behaviour around 300 K. Fig. 11 shows the double logarithmic plot of the frequency dependence of ε' and ε'' for BT(9.1)/PDMS at 290 K. Fig. 12 shows the dependence of ε' and ε'' on $BaTiO_3$ content for the BT/t-PDMS-10 systems. Two mechanisms for the dielectric dispersion are expected: one is the orientational relaxation of $BaTiO_3$ particles and the other is the interfacial electrode polarization due to impurity ions contained in the system. If the latter is the main mechanism, the slope of $\log \varepsilon''$ versus $\log f$ curve should be -1 in the low-frequency region since the contribution of ionic conductivity to the loss is inversely proportional to frequency. In Figs. 11 and 12, the slope is much lower than -1. We also found that the dielectric behaviour was independent of the distance between electrodes. Therefore, the mechanism of interfacial polarization can be ruled out.

As is seen in Fig. 11, ε' depends not only on the content of $BaTiO_3$ but also on the viscosity of PDMS. This can be explained easily by assuming the orientational dielectric dispersion of the particles having the dipole moment, i.e. in a medium of low viscosity, the particles of $BaTiO_3$ can reorient in the direction of an alternating electric field but in a high-viscosity medium, $BaTiO_3$ particles cannot reorient. Thus the strong dielectric relaxation seen in Figs. 11 and 12 can be attributed to reorientation of $BaTiO_3$ particles having strong dipole moment. We see that the relaxation time is too long to observe the dielectric loss maximum even for the PDMS medium with the lowest viscosity. As described previously, this assignment was also confirmed from the dielectric data on the crosslinked PDMS containing $BaTiO_3$, specifically, the matrix t-PDMS-10 of BT(13.7)/t-PDMS-10 was crosslinked [28]. The data indicated that high

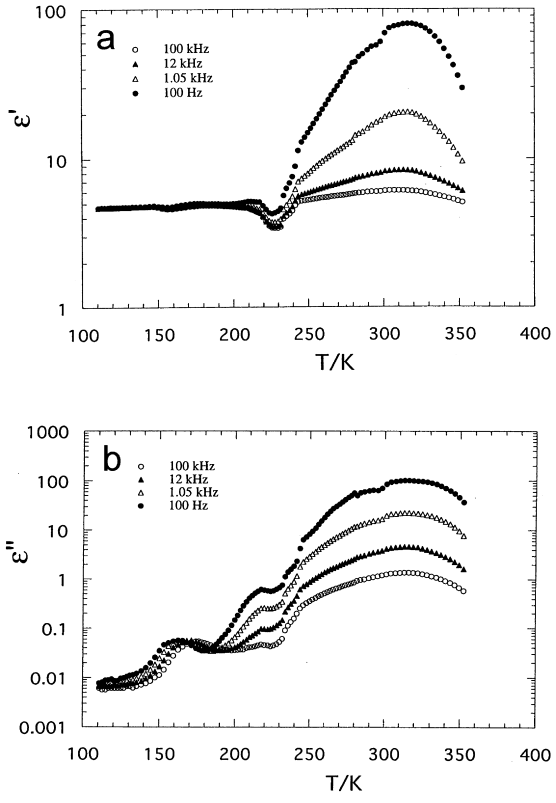

Fig. 10. Temperature dependence of dielectric constant ε' (a) and loss factor ε'' (b) for BT(9.1)/t-PDMS-10 at frequencies given in the figure.

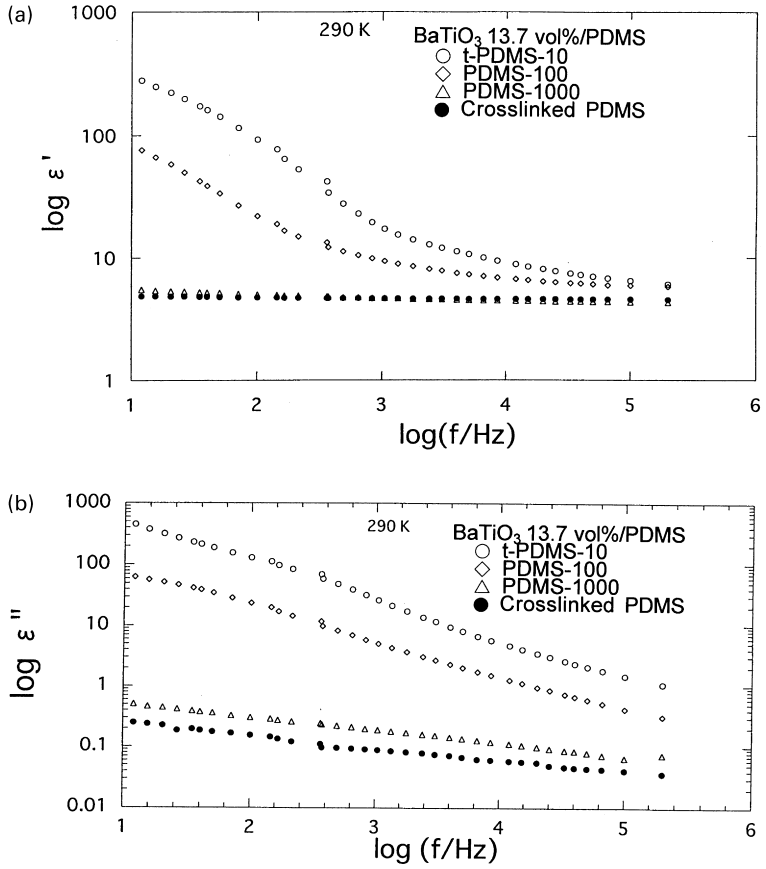

Fig. 11. Double logarithmic plot of dielectric constant ε' (a) and loss factor ε'' (b) at 290 K for suspensions of $BaTiO_3$ in PDMSs of various viscosities.

ε' observed in the system before crosslinking was no longer seen after crosslinking as the reorientation of the particles was not allowed in the elastomer.

3.2.3. Relaxation time and relaxation strength

In order to examine the mobility of $BaTiO_3$ particles, we also carried out dielectric measurements in the low-frequency region from 0.005 to 10 Hz. Results for BT(1.6)/t-PDMS-10 and for BT(9.1)/t-PDMS-10 are shown in Fig. 13a and b, respectively. In the former system, the content of $BaTiO_3$ is only 1.6 vol% and hence the particles do not form a network structure. As shown in this figure, no loss maximum can be seen in our experimental window of the range above 10^{-3} Hz.

According to Debye, the dielectric relaxation time τ of a spherical particle suspended in a viscous medium of viscosity η is given by (see e.g. Ref. [29])

$$\tau = \frac{4\pi\eta a^3}{k_B T} \tag{5}$$

where a is the radius of the particle. As described in the experimental section, the $BaTiO_3$ particles used in the present study has a shape close to sphere or cube, and the diameter is distributed between 0.1 and 0.5 μm. Therefore, we assumed that the $BaTiO_3$ particles are spherical and calculated τ to be 0.38 and 48 s for the diameter of the particle of 0.1 and 0.5 μm, respectively. These relaxation times correspond to the loss maximum frequencies of 1.5 and 0.03 Hz, respectively. As seen in Fig. 13a, no loss maximum is seen in this range. This indicates that the $BaTiO_3$ particles do not move independently but form aggregates or clusters, and therefore the relaxation time becomes longer than that for single particle. In order to check whether the value of high dielectric constant observed in low frequency is consistent with the dipole moment of the $BaTiO_3$ particles, we calculated the dielectric relaxation strength $\Delta\varepsilon$ by the Onsager–Kirkwood equation (in SI unit) [30]:

$$\Delta\varepsilon = \frac{Ng\mu^2}{3k_B T\varepsilon_0}\left(\frac{\varepsilon_U + 2}{3}\right)^2\left(\frac{3\varepsilon_R}{2\varepsilon_R + 1}\right) \tag{6}$$

where N is the number of particles in unit volume, g the Kirkwood correlation parameter, $k_B T$ the thermal energy, ε_0 the absolute dielectric constant of vacuum, μ the dipole moment, ε_U the unrelaxed dielectric constant and ε_R the relaxed dielectric constant. As discussed in Section 3.1.1, μ of a $BaTiO_3$ particle with the size of 0.3 μm is estimated to be 4.3×10^{-21} Cm ($=1.3\times10^{9}$ D). The number of the $BaTiO_3$ particles (N) is 1.5×10^{11}. From these data, we calculated $\Delta\varepsilon$ of BT(1.8)/t-PDMS-10 to be 2.1×10^{8} assuming $g = 1$. High-frequency dielectric constant ε_U is 5.0 and is much smaller than $\Delta\varepsilon$.

In Fig. 13a for the dilute suspension, it appears that the

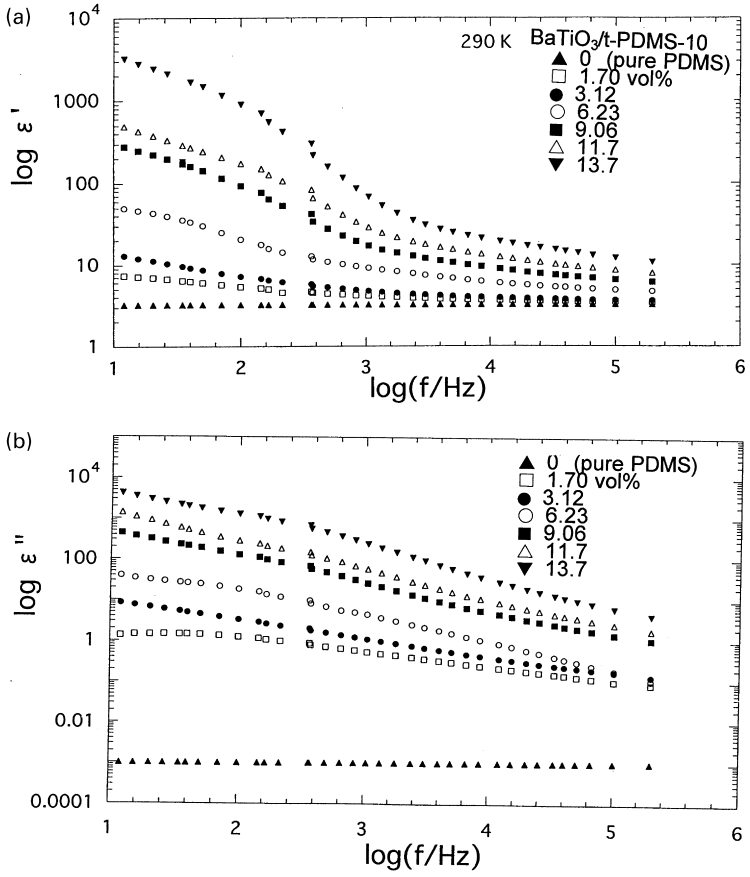

Fig. 12. Dielectric constant ε' (a) and loss factor ε'' (b) for suspensions with various contents of $BaTiO_3$.

loss maximum locates below 0.001 Hz and it is difficult to determine $\Delta\varepsilon$ by the routine methods of analysis. Therefore, we roughly estimated the order of $\Delta\varepsilon$ neglecting the distribution of relaxation times as follows. The Debye equation of dielectric relaxation predicts that in the region of $\omega\tau \gg 1$, $\varepsilon' - \varepsilon_U \sim \Delta\varepsilon/\omega^2\tau^2$ and $\varepsilon'' \sim \Delta\varepsilon/\omega\tau$ where ω is the angular frequency and τ the average relaxation time. Then $\Delta\varepsilon$ is given by $\varepsilon''^2/(\varepsilon' - \varepsilon_U)$. From the experimental ε' and ε'' data at 0.01 Hz, $\Delta\varepsilon$ for BT(1.6)/t-PDMS becomes 3900. The much lower value of $\Delta\varepsilon$ than the calculated value with $g = 1$ may be explained by considering two mechanisms. One is that there are several polarization domains in the single particle and the dipole moment of the particle is not so high as discussed in Section 3.1.1. The second is that the dipoles tend to orient anti-parallel resulting in the value of g in Eq. (6) less than unity.

Similar analysis for BT(9.1)/t-PDMS-10 (Fig. 13b) resulted in the theoretical $\Delta\varepsilon = 1.1 \times 10^9$ while the observed $\Delta\varepsilon = 5.7 \times 10^6$. The difference can be explained as above.

3.2.4. Rheo–dielectric behaviour

In order to get further information of the internal structure of aggregates, we carried out dielectric measurements in a shear flow. Fig. 14 shows the shear rate dependence of ε' at 1 kHz for suspensions containing 13.7, 9.1 and 3.12 vol% of $BaTiO_3$. It is noted that we applied relatively high shear rate compared with the viscosity measurements. It is seen that ε' decreases dramatically with increasing shear rate. This behaviour is the reverse of our expectation. We expected before rheo–dielectric measurements that the ε' will increase in a shear field since aggregates break up and the mobility of particles increases.

We explain the result as follows. At the stationary state, chain-like aggregates have a coiled structure as discussed above. These aggregates are broken into smaller size under a shear field, and at the same time they are extended in the direction of shear. Thus the rotational relaxation time increases much with increase of average radius of inertia Fig. 15. Thus dielectric response cannot be observed in a shear field.

When flow was stopped, ε' recovered gradually to the value at the stationary state. When the shear rate was changed stepwise, a transient change of ε' was also observed. We see that the recovery of ε' occurs through two processes, namely the fast and slow, as observed for the viscosity measurements. Fig. 16 shows the analyses of the transient variation of ε' in terms of the retardation equation similar to Eq. (3). The time constants for the slow and fast processes are 10 and 300 ± 100 s, respectively. These values agree well with those for the transient change of viscosity. Therefore, the transient change of ε' reflects the structural reorganization of aggregates.

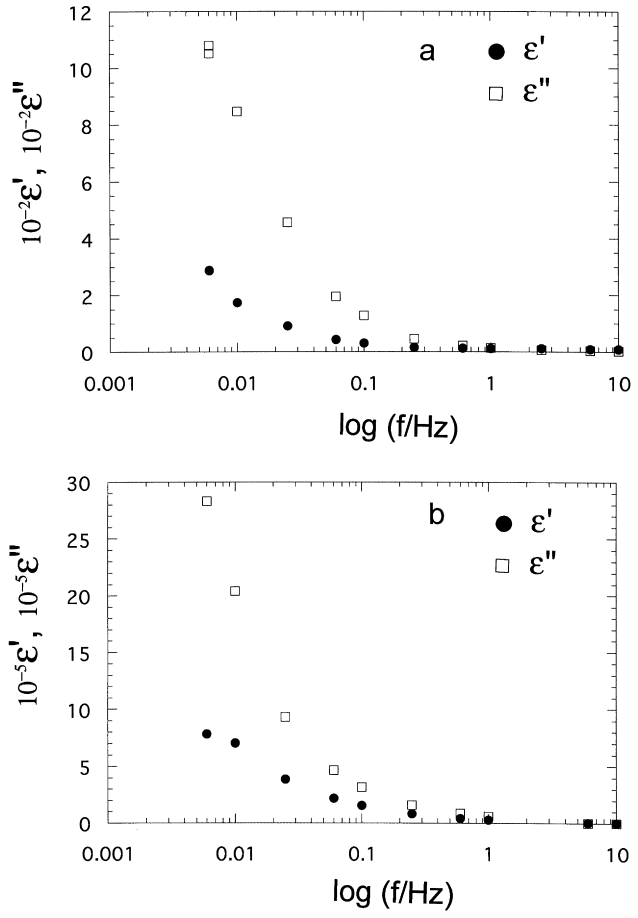

Fig. 13. Frequency dependencies of ε' and ε'' for in the low-frequency range for: (a) BT(1.6)/t-PDMS-10; and (b) BT(9.1)/t-PDMS-10. It is noted that the values of ε divided by 10^{α} are plotted for: (a) $\alpha = 2$; and (b) $\alpha = 5$.

Fig. 17 illustrates the structural change of aggregates schematically. In the stationary state (A), aggregates have a coiled chain-like conformation. In a shear field (B), the chains are broken into smaller ones and stretched in the direction of the shear field. When shearing is stopped, the stretched chains tend to take a coiled conformation. The recovery from B to A is achieved through two processes. The fast process has a time constant of ca 10 s and probably corresponds to the recovery from the extended structure to the coiled one as illustrated in Fig. 17, i.e. the change from B to C. Then the aggregates continue the reorganization of particles to attain more stable network structures, i.e. the change from C to A. This slow process will need longer time, because in this process the part of the aggregate is broken and recombine to the other coiled aggregates. The activation energy is approximately given by Eq. (2) and is much higher than thermal energy.

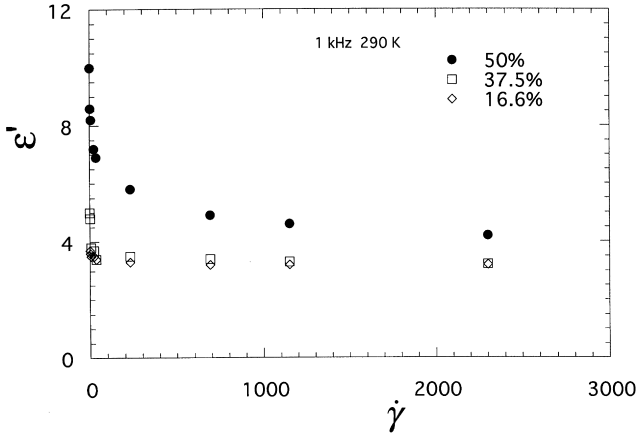

Fig. 14. Shear rate dependence of ε' for suspensions of t-PDMS containing various amount of $BaTiO_3$ indicated in the figure.

4. Conclusions

Suspensions of $BaTiO_3$/PDMS exhibit non-linear viscoelastic behaviour such as shear thinning, thixotropy and rheopexy. The viscoelastic behaviour can be explained by assuming the shear rate dependence of the size and structure of aggregates of $BaTiO_3$ particles. There are at least two processes for the transient change of viscosity. The time constants for the fast and slow processes are 10 and 200 s, respectively.

The system containing $BaTiO_3$ more than 10 vol%

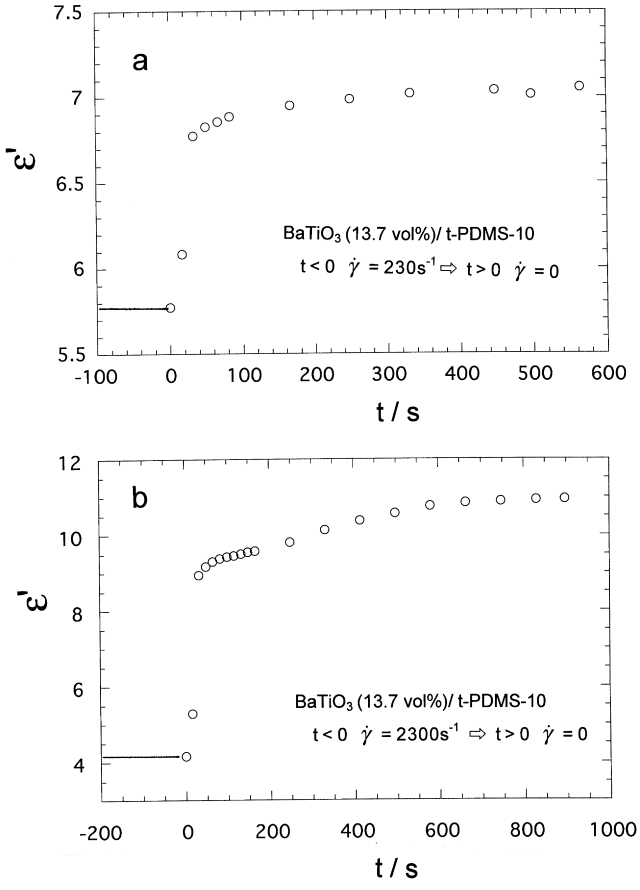

Fig. 15. Time dependence of ε' after stop of shearing for BT(13.7)/t-PDMS. Shear rate in the range of $t < 0$ was: (a) 230 s^{-1}; and (b) 2300 s^{-1}.

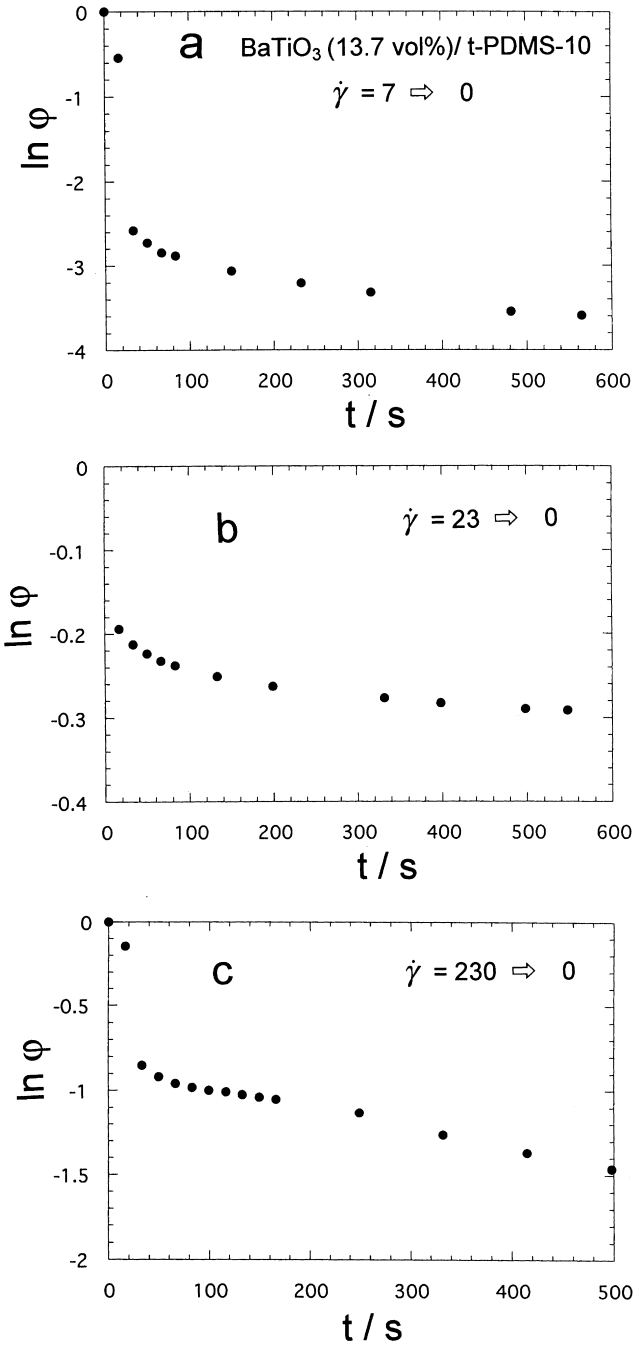

Fig. 16. Analyses of the time dependence of ε' after sudden stop of shearing based on an equation similar to Eq. (3). Here $\varphi = [\varepsilon'(t) - \varepsilon'(\infty)]/[\varepsilon'(0) - \varepsilon'(\infty)]$. $\dot{\gamma}$ in the range of $t < 0$: (a) is 7; (b) 23; and (c) 230 s^{-1}.

exhibits plasticity and second plateau in dynamic shear modulus. The shear rate dependence of the stress conformed to the Casson equation. The results suggest that at high concentration of $BaTiO_3$, the particles form a network structure.

Dielectric relaxation due to reorientation of $BaTiO_3$ particles was observed. The dielectric relaxation region shifts

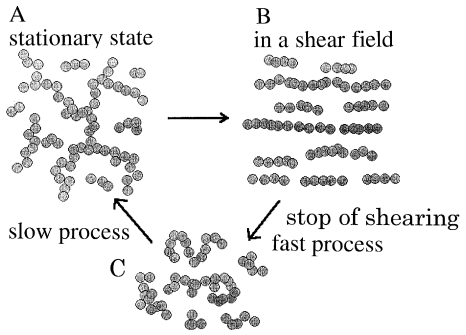

Fig. 17. Schematic representation of the structures of aggregates of $BaTiO_3$ in suspensions: (A) the stationary state; (B) in a shear field; and (C) after shearing is stopped.

to lower frequency with increasing viscosity of the matrix PDMS. Both of the estimated relaxation time and the relaxation strength indicate that the particles form aggregates. The relaxation strength also indicates that the dipoles are mostly arranged anti-parallel.

Under a shear field, the dielectric constant decreases. Stepwise change of the shear rate also causes the recovery of ε'. The recovery reflects the change in the structure of the aggregates and occurs in two steps. The time constants for the fast and slow processes are 10 and 300 s, respectively, in rough agreement with the time constants for the transient change of viscosity.

Present data as well as the data reported in literature suggest that $BaTiO_3$ particles are linked linearly by the dipole–dipole interactions. In the stationary state, the aggregates have a coiled conformation but is stretched in a shear field.

Acknowledgements

D.K. is grateful for a fellowship from the Japan Society for the Promotion of Science (JSPS).

References

[1] Bingham EC. Fluidity and plasticity. New York: McGraw-Hill, 1922.
[2] Mill CC, editor. Rheology of disperse systems New York: Pergamon, 1959.
[3] Onogi S, Matsumoto T. Polym Engng Rev 1981;1:45.
[4] Tirado-Mirande M, Schmitt A, Callejas-Fernandez J, Fernandez-Barbero A. Progr Colloid Polym Sci 1997;104:138.
[5] Shaw DT. Introduction to colloid and surface chemistry. London: Butterworths, 1980.
[6] Russel WD, Saville DA, Schowalter WR. Colloid dispersions. Cambridge: Cambridge University Press, 1989.
[7] Otsubo Y, Watanabe K. J Colloid Interface Sci 1989;127:214.
[8] Doi M, Chen D. J Chem Phys 1989;90:5271.
[9] Chen D, Doi M. J Chem Phys 1989;91:2656.
[10] Jona F, Shirane G. Ferroelectric crystals. New York: Pergamon Press, 1962.
[11] Merz WJ. Phys Rev 1949;76:1221.
[12] Adachi K, Fukui F, Kotaka T. Langmuir 1994;10:126.
[13] Batchelor GK. J Fluid Mech 1977;83:97.

[14] Tsenoglou C. J Rheol 1990;34:15.
[15] Collins IR. J Colloid Interface Sci 1996;178:361.
[16] Ito Y, Shishido S. J Polym Sci: Phys Ed 1973;11:2283.
[17] Yang IK, Shine AD. J Rheol 1992;36:1079.
[18] Saluena C, Rubi JM. J Chem Phys 1995;102:3812.
[19] Winslow WM. J Appl Phys 1949;20:1137.
[20] Koyama K, Minagawa K, Watanabe T, Kumakura Y, Takimoto J. J Non-Newtonian Fluid Mech 1995;58:195.
[21] Koyama K. Int J Mod Phys B 1996;10:3067.
[22] See H, Doi M. J Phys Soc Jpn 1991;60:2778.
[23] Chantrell RW, Bradbury A, Popplewell J, Charles SW. J Appl Phys 1982;53:2743.
[24] Casson N. In: Mill CC, editor. Rheology of disperse systems, New York: Pergamon Press, 1959. p. 84.
[25] Matsumoto T, Takashima A, Masuda T, Onogi S. Trans Soc Rheol 1970;14:617.
[26] Onogi S, Matsumoto T, Warashina Y. Trans Soc Rheol 1973;17:175.
[27] Adachi H, Adachi K, Ishida Y, Kotaka T. J Polym Sci: Polym Phys Ed 1979;17:851.
[28] Khastgir D, Adachi K. J Polym Sci B: Polym Phys Ed 1999;37:3065.
[29] McCrum NG, Read BE, Williams G. Anelastic and dielectric effects in polymeric solids. New York: Wiley, 1967. chap. 5.
[30] McCrum NG, Read BE, Williams G. Anelastic and dielectric effects in polymeric solids. New York: Wiley, 1967. chap. 3.